Does the degree of coarctation of the aorta influence wall shear stress focal heterogeneity?

John Gounley[1], Rafeed Chaudhury[2], Madhurima Vardhan[1], Michael Driscoll[3], Girish Pathangey[2], Kevin Winarta[2], Justin Ryan[4], David Frakes[2], and Amanda Randles[1]

***Abstract*— The development of atherosclerosis in the aorta is associated with low and oscillatory wall shear stress for normal patients. Moreover, localized differences in wall shear stress heterogeneity have been correlated with the presence of complex plaques in the descending aorta. While it is known that coarctation of the aorta can influence indices of wall shear stress, it is unclear how the degree of narrowing influences resulting patterns. We hypothesized that the degree of coarctation would have a strong influence on focal heterogeneity of wall shear stress. To test this hypothesis, we modeled the fluid dynamics in a patient-specific aorta with varied degrees of coarctation. We first validated a massively parallel computational model against experimental results for the patient geometry and then evaluated local shear stress patterns for a range of degrees of coarctation. Wall shear stress patterns at two cross sectional slices prone to develop atherosclerotic plaques were evaluated. Levels at different focal regions were compared to the conventional measure of average circumferential shear stress to enable localized quantification of coarctation-induced shear stress alteration. We find that the coarctation degree causes highly heterogeneous changes in wall shear stress.**

I. Introduction

Despite treatment, coarctation of the aorta (CoA) is associated with higher morbidity and complications such as early onset atherosclerosis than found in the average population. According to the 2016 American Heart Association Statistical Update, CoA is among the most prevalent congenital heart defects (7.6%), affecting more than 75,000 people in the U.S. The disease is characterized by presence of a constricted segment of the descending thoracic aorta (dAo).

Previous studies have shown that atherosclerosis in the dAo develops in regions exposed to low wall shear stress, the tangential force per unit area exerted on the vasculature from local hemodynamics. Specifically, localized differences in wall shear stress (WSS) indices have been suggested to indicate location of likely atherosclerotic plaque development and progression [4], [7], [13]. With respect to the general population, Markl *et al.* found that plaques in the dAo were focused on the inner curvature and observed a statistically significant difference in WSS indices of patients with and without plaques. Among studies of CoA, LaDisa *et al.* created computational models of stents implanted in CoAs and used CFD to compare their effects on WSS-related metrics in the dAo [3], [5]. Marked variations in time-averaged WSS were shown downstream of dAo depending on the type of stent implanted in coarctation surgeries. Likewise, a comparative study revealed localized differences in time-averaged wall shear stress (TAWSS) within dAo of surgically treated CoA patients and control subjects [4]. Timmins *et al.* evaluated the potential pitfalls of TAWSS and circumferentially averaged WSS as markers for disease. They demonstrated the statistical relevance of using a spatial breakdown instead of averages in the coronary arteries [13].

While there is, therefore, considerable evidence to support the conclusion that the vascular geometry influences not only hemodynamic risk factors like WSS but the associated focal heterogeneity, the influence of the degree of coarctation on localized differences in WSS indices has yet to be full established. An understanding of coarctation-induced shear stress alterations may have a future role in the diagnosis or treatment of known co-morbidities of CoA.

We hypothesized that the degree of coarctation will influence the focal WSS heterogeneity such that averaged values could not capture. As a case study to motivate future research, we use computational fluid dynamic simulations and *in vitro* experiment to quantitatively evaluate flow profiles and the distribution of WSS in the dAo in geometries representing a range of coarctation degrees for one patient-specific aorta. The study was restricted to one representative geometry to control for flow modification caused by other topological variances found in the normal patient population.

The contributions of this study are: (1) validation of a massively parallel computational model against experimental results for the patient geometry, confirming the ability to accurately simulate flow in complex geometries at high Reynolds number; (2) a quantitative evaluation of local shear stress patterns for a range of degrees of coarctation, by considering WSS patterns at two cross sectional slices prone to develop atherosclerotic plaques; and (3) a study of WSS levels at different focal regions as opposed to average circumferential WSS. Our results indicate that the circumferentially averaged WSS fails to account for important WSS changes per focal region, particularly proximal to the coarctation.

II. Methodology

A. Computational fluid model

Computational simulations are conducted using HARVEY, a massively parallel computational fluid dynamics code

1. Department of Biomedical Engineering, Duke University, Durham, NC
2. Department of Biomedical Engineering, Arizona State University, Tempe, AZ
3. Computer Science Division, University of California, Berkeley, CA
4. Phoenix Children's Hospital, Phoenix, AZ

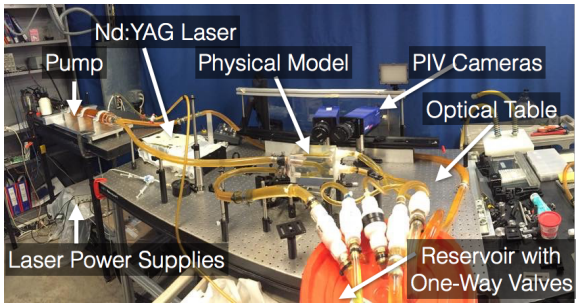

Fig. 1: Photograph of *in vitro* flow loop

which implements the lattice Boltzmann method (LBM). Based on kinetic theory, LBM is an alternate approach to solving the standard Navier-Stokes equations governing fluid flow. Instead of solving directly for velocity and pressure, LBM represents fluid by a probability distribution function f of particles, which move at discrete velocities around a fixed Cartesian lattice. The time evolution of f is governed by the lattice Boltzmann equation:

$$f_i(\mathbf{x}+\mathbf{c}_i\delta t, t+\delta t) - f_i(\mathbf{x},t) = -\Omega\Big(f_i(\mathbf{x},t) - f_i^{eq}(\mathbf{x},t)\Big).$$

A comprehensive explanation of LBM may be found in [12]. The HARVEY implementation uses the standard three-dimensional D3Q19 velocity discretization and the single relaxation time BGK collision kernel Ω. A no-slip boundary condition is enforced on the rigid vessel walls by the halfway bounce-back method, while finite difference boundary conditions are used at the inlets and outlets [6]. Transverse WSS is computed from WSS using the definition of secondary WSS in [8]. Further details about the numerical implementation, parallelization, and scaling of HARVEY can be found in [9], [10].

To simplify the experimental design for this case study, we assume that vessel walls are rigid and consider a steady flow. Based on the high shear rate in the aorta, the flow is modeled as Newtonian. Simulations were conducted with HARVEY at 100μm resolution, based on results of a convergence test.

B. Physical fluid model

Experiments were conducted in a flow loop driven by a custom computer-controlled piston pump described in an earlier study [2]. The flow loop had three major components: the piston pump, an optically clear physical urethane CoA model, and a reservoir tank to receive the flow from each of the outlets, as in figure 1.

The CoA model was connected to the flow loop with flexible Tygon tubing (R-3603, Ryan Herco Flow Solutions, Burbank, CA) and placed on a custom stage to allow a laser light sheet to pass vertically through the model centerplane for optical imaging. The fluid flowing through the loop was a sodium iodide-based solution ($\nu = 2.05\times10^{-6}$ m^2/s) with a refractive index matched to the urethane block ($n = 1.49$), to render the urethane wall invisible and eliminate optical distortion during particle image velocimetry (PIV).

Velocity fields on a plane passing through the center of the model were captured using PIV. A LaVision 3D Flowmaster PIV system was used (LaVision, Ypsilanti, MI, USA) and consisted of two 1,476 $\times$ 1,040 pixel Imager Intense PIV CCD cameras with 6.45μm square pixels. The cameras were fitted with AF Micro-Nikkor 60mm lenses (Nikon, Tokyo, Japan) with lens f numbers of 8 and were placed in a stereographic configuration centered approximately 55D downstream of the inlet. A 532nm Gemini PIV dual cavity double-pulsed Nd:Yag laser (New Wave Research, Fremont, CA, USA) and various optics formed a 0.5mm thick, double pulsed, vertical light sheet focused at the centerline of the model for both the CoA and model inlet regions. In the laser sheet, light was scattered by silver coated hollow glass spheres (TSI Incorporated, Shoreview, MN, USA) having a mean diameter between 8-12μm and a density listed at 1.65 g/mL. The system operated in two frame cross-correlation mode, and standard stereo PIV procedures were followed to obtain low-noise measurements of particle displacement and velocity with a high percentage ($> 95\%$) of valid vectors [1]. Acquisition for steady flow comprised of a minimum of three trials resulting in a minimum of 200 image pairs.

III. Results

A. Validation

A standard method for the validation of a CFD application is the simulation of flows for which the incompressible Navier-Stokes equations have analytic results, such as Womersley and Dean flows. When focusing on simulating blood flow in vascular geometries, such flows may not fully reflect the challenges of the specific problem and provide a comprehensive assessment of stability and validity. For instance, a simulation of flow through a CoA must accurately resolve the narrow branches of the aortic arch and handle the high Reynolds numbers. A comparison with experimental results for a physiologically relevant flow in a vascular geometry resolves this deficiency. 3D-printing allows the same geometry to be used for computation and experiment.

A comparison between HARVEY and *in vitro* experiment was conducted to validate the HARVEY code for flow in a CoA. We consider a patient-specific CoA geometry with a 65% reduction in cross-sectional area at the coarctation [11], using the same geometry for *in vitro* experiment and HARVEY. A constant flow rate of approximately 5000 mm^3/s was imposed at the inlet and a zero pressure boundary condition governed the outlets. The magnitude of the velocity $\mathbf{v}$ through the coarctation was recorded; corresponding slices from *in vitro* and HARVEY are shown in figure 2. With a RMSD=0.042 between average velocity magnitudes in simulation and experiment (figure 2, bottom), HARVEY successfully resolves the experimental flow pattern both coming from the aortic arch and through the CoA, in qualitative and quantitative respects. As the strain rate tensor $S = (1/2)(\nabla\mathbf{v} + (\nabla\mathbf{v})^T)$ is used in HARVEY to compute stress $\sigma_{\alpha\beta}$, this comparison supports the accuracy of the WSS computation within HARVEY as well.

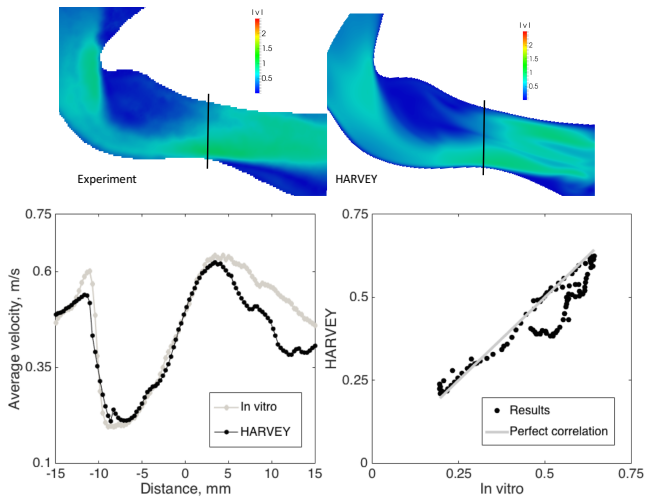

Fig. 2: Magnitude of velocity through coarctation, from *in vitro* experiment (top left) and HARVEY (top right). Average velocity over vertical slices of the images above, along the vessel (bottom left) and directly compared (bottom right).

B. WSS dependence on coarctation degree

From the CoA with a 65% coarctation used in the preceding validation comparison, we used the graphics software Blender to construct a range of geometries with 55, 47, 40, 30, 20, 10, and 0% coarctations. To facilitate the comparison between the degrees of coarctation, a constant inflow rate of 4712.3 mm^3/s was enforced at the inlet, while zero pressure condition governed the outlets. To represent blood flow in large vessels, a Newtonian fluid was simulated with a dynamic viscosity of 3.75cP. The model was simulated with HARVEY until the system reached steady-state.

WSS was computed over two slices of the dAo, proximal and distal to the coarctation, as indicated in figure 3. Following the approach from [13], each slice was divided into four focal regions; WSS was averaged over the entire circumference and over each individual focal region. Regions 3 and 1 lie on the inner and outer curvature of the dAo, respectively. Dividing the slice into focal regions allows an evaluation of the focal WSS heterogeneity.

Figures 4 & 5 show the percentage changes in WSS and transverse WSS, relative to the 0% coarctation, at distal and proximal slices, respectively. In the distal slice, we anticipated little difference between focal regions, with the remaining variation due to the vessel curvature, rather than coarctation degree. This hypothesis proved broadly true, with insignificant changes of 5% or less in most instances, but certain coarctation degrees produced somewhat larger variation in WSS in a given region. It is observed that these variations are overwhelmingly due to changes in transverse WSS, whereas axial WSS is virtually constant within a given focal region over the entire range of coarctations simulated (axial WSS data not shown). Thus, the circumferential average is a reasonable reflection of WSS within each focal region, though it fails to completely account for region-level changes at certain coarctation degrees which may produce low WSS.

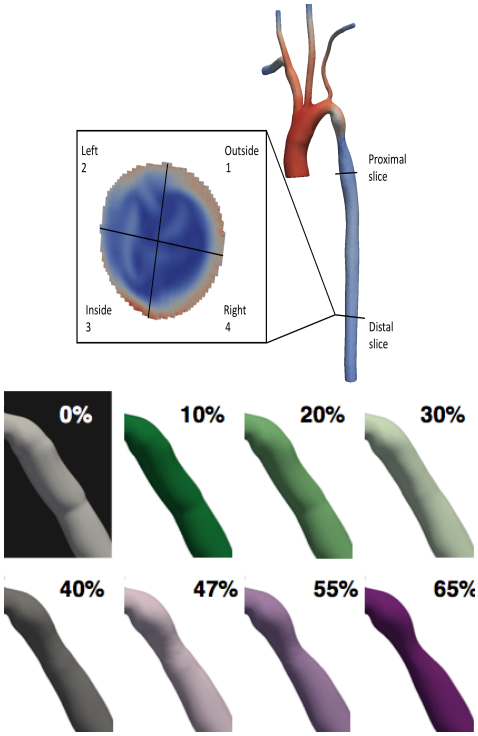

Fig. 3: Regions 1-4 of each slice, with color indicating WSS (top left). Locations of slices proximal and distal to the coarctation, with color indicating pressure (top right). Range of 0-65% coarctations used in simulations (bottom).

We expected that the coarctation would have a larger impact on WSS in the region of the dAo proximal to the coarctation, as the flow profile is still disrupted from its passage through the coarctation, and this larger impact is clear in figure 5. As the coarctation degree increased, so also did the change in circumferentially averaged WSS and transverse WSS increase. However, these average values fail to reflect the substantial and varied changes in WSS per focal region, which are caused by the location of non-axisymmetric and disturbed flow profile emanating from the coarctation. For instance, at 20% coarctation, the change in circumferentially averaged WSS was insignificant, despite showing changes of 20% or more in all four regions. The disagreement with the circumferential average was qualitative as well: for while change in regions 3 and 4 was somewhat qualitatively consistent with the circumferential average, regions 1 and 2 displayed much more non-linear relationships between WSS change and coarctation degree. The relationship between changes in WSS versus transverse WSS also requires consideration of the focal regions: the circumferential averages are qualitatively very similar, but this does not remain true when considering region 2.

IV. Discussion & Conclusion

We have presented a case study evaluating the influence that the degree of coarctation has on subsequent WSS patterns in the dAo. The CFD code used in the study was validated in the patient-specific vascular geometry and

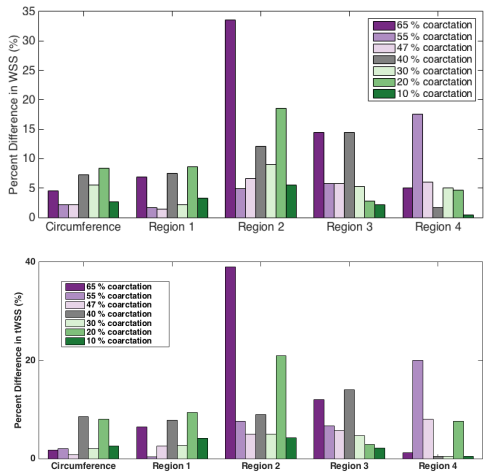

Fig. 4: For a distal slice of dAo, percentages changes in WSS (above) and transverse WSS (below) at a range of degrees of coarctation, relative to the aorta with no coarctation. Results are averaged circumferentially and over regions 1-4.

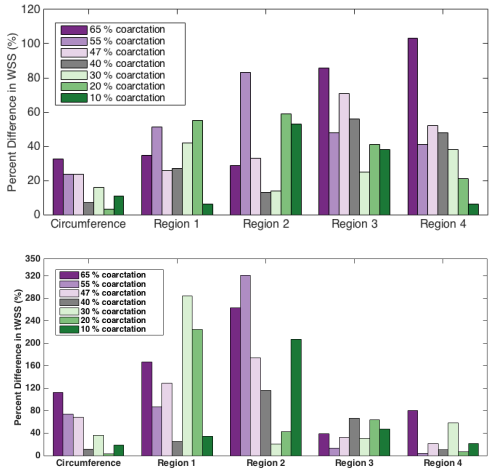

Fig. 5: For a proximal slice of dAo, percentages changes in WSS (above) and transverse WSS (below) at a range of degrees of coarctation, relative to the aorta with no coarctation. Results are averaged circumferentially and over regions 1-4.

flow regime through comparison with data obtained from *in vitro* experiments. We found that changing the coarctation degree could significantly change WSS and transverse WSS on the focal region level, to an extent that could not be observed from the circumferentially averaged results. The local changes in WSS did not depend linearly on coarctation degree, nor were they confined to one or two focal regions. Instead, the alteration of the flow pattern produced by the coarctation degree could cause heterogeneous changes in WSS indices over the entire circumference. Further, these differences occurred both proximal and distal to the coarctation, though they decrease in the distal location. As the local changes in WSS indices are substantially higher than the circumferentially averaged change, it is clear that investigations of the influence of coarctation-induced shear stress alterations on adverse hemodynamic risk factors must account for their spatial heterogeneity. The large localized differences in WSS indices may indicate regions especially susceptible to the development of plaques and could motivate future investigations for diagnoses and treatment.

V. Acknowledgments

The authors would like to thank Liam Krauss, Lawrence Livermore National Laboratory, for assistance with visualization.

Research reported in this publication was supported by the Office Of The Director, National Institutes Of Health of the National Institutes of Health under Award Number DP5OD019876. The content is solely the responsibility of the authors and does not necessarily represent the official views of the National Institutes of Health.

Computing support for this work came from the Lawrence Livermore National Laboratory (LLNL) Institutional Computing Grand Challenge program. This work was partially supported by supported by an LLNL LDRD-15-LW-029 grant. The work was performed under the auspices of the United States Department of Energy by the University of California, Lawrence Livermore National Laboratory Contract W-7405-Eng-48.

References

[1] R. J. Adrian and J. Westerweel. *Particle Image Velocimetry*, volume 30. Cambridge University Press, 2010.

[2] R. A. Chaudhury, V. Atlasman, G. Pathangey, N. Pracht, R. J. Adrian, and D. H. Frakes. A high performance pulsatile pump for aortic flow experiments in 3-dimensional models. *Cardiovasc. Eng. Technol.*, 7(2):148–158, 2016.

[3] S. Kwon, J. A. Feinstein, R. J. Dholakia, and J. F. LaDisa Jr. Quantification of local hemodynamic alterations caused by virtual implantation of three commercially available stents for the treatment of aortic coarctation. *Pediatr. Cardiol.*, 35(4):732–740, 2014.

[4] J. LaDisa, F. John, R. J. Dholakia, C. A. Figueroa, I. E. Vignon-Clementel, F. P. Chan, M. M. Samyn, J. R. Cava, C. A. Taylor, and J. A. Feinstein. Computational simulations demonstrate altered wall shear stress in aortic coarctation patients treated by resection with end-to-end anastomosis. *Congenit. Heart Dis.*, 6(5):432–443, 2011.

[5] J. F. LaDisa, C. A. Taylor, and J. A. Feinstein. Aortic coarctation: recent developments in experimental and computational methods to assess treatments for this simple condition. *Prog. Pediatr. Cardiol.*, 30(1):45–49, 2010.

[6] J. Latt, B. Chopard, O. Malaspinas, M. Deville, and A. Michler. Straight velocity boundaries in the lattice Boltzmann method. *Phys. Rev. E*, 77(5):056703, 2008.

[7] M. Markl, S. M. Brendecke, J. Simon, A. J. Barker, C. Weiller, and A. Harloff. Co-registration of the distribution of wall shear stress and 140 complex plaques of the aorta. *Magn. Reson. Imaging*, 31(7):1156–1162, 2013.

[8] U. Morbiducci, D. Gallo, S. Cristofanelli, R. Ponzini, M. A. Deriu, G. Rizzo, and D. A. Steinman. A rational approach to defining principal axes of multidirectional wall shear stress in realistic vascular geometries, with application to the study of the influence of helical flow on wall shear stress directionality in aorta. *J. Biomech.*, 48(6):899–906, 2015.

[9] A. Randles, E. W. Draeger, and P. E. Bailey. Massively parallel simulations of hemodynamics in the primary large arteries of the human vasculature. *J. Comp. Sci.*, 9:70–75, 2015.

[10] A. Randles, E. W. Draeger, T. Oppelstrup, L. Krauss, and J. A. Gunnels. Massively parallel models of the human circulatory system. In *Proc. International Conference for High Performance Computing, Networking, Storage and Analysis*, page 1. ACM, 2015.

[11] A. P. Randles, M. Bächer, H. Pfister, and E. Kaxiras. A lattice Boltzmann simulation of hemodynamics in a patient-specific aortic coarctation model. In *Statistical Atlases and Computational Models of the Heart. Imaging and Modelling Challenges*, pages 17–25. 2012.

[12] S. Succi. *The lattice Boltzmann equation: for fluid dynamics and beyond*. Oxford University Press, 2001.

[13] L. H. Timmins, D. S. Molony, P. Eshtehardi, M. C. McDaniel, J. N. Oshinski, H. Samady, and D. P. Giddens. Focal association between wall shear stress and clinical coronary artery disease progression. *Ann. Biomed. Eng.*, 43(1):94–106, 2015.